Physics of the Solid State, 2024, Vol. 66, No. 10

03,08

Multilayer selective sensor structures based on nonstoichiometric oxides of manganese and tin

© *V.V. Bolotov, E.V. Knyazev*¶, *S.N. Nesov, K.E. Ivlev, I.V. Ponomareva, Yu.A. Stenkin, E.A. Roslikova, D.V. Sokolov*

Omsk Scientific Center of the Siberian Branch of the Russian Academy of Sciences,
Omsk, Russia
¶ E-mail: knyazevyegor@mail.ru

Received July 16, 2024
Revised August 10, 2024
Accepted August 11, 2024

The morphology, chemical composition of nonstoichiometric manganese oxide obtained by various methods for its use as a sorbing layer are investigated. The changes in the chemical state of manganese after interaction with hydrogen sulfide vapors have been studied. The differences in the sorption mechanism for layers obtained by different technological modes are shown. The possibility of creating a test sensor structure with a sorbing layer based on manganese and tin oxides is demonstrated.

Keywords: gas sorbents, gas sensors, manganese oxide, tin oxide.

DOI: 10.61011/PSS.2024.10.59619.203

1. Introduction

Problem of concentration determination of elements of pollutants and harmful impurities in atmosphere and ready products is actual for ecology, technological processes monitoring and labour safety. There is need to create devices able to register small concentrations of contaminating compounds, having at this stability and selectivity. Class of most widely occurred technological pollutants includes sulphur compounds (H_2S, SO_2 etc.), nitrogen compounds (NH_3, NO_2) [1–6]. To remove sulfur-containing impurities from the gaseous phase sorbents based on metal oxides (MnO, CaO, ZnO, V_2O_3 etc.) are widely used [1,5–8], at that bonding of sour gas running chemical reactions on sorbent surface. The manganese oxide is rather promising material for use as sorbent, it has high activity during interaction with sulfur-containing and nitrogen compounds, and high sorption capacity [1–7]. So, the objective of increasing selectivity and sensitivity of resistive gaseous sensors can be solved using manganese oxide layers as filtering and sorption components. In such configuration the multilevel vertically integrated sensor structure is formed, it comprises filtering, sorption and sensitive layers.

In this paper we studied the morphology, chemical and elemental composition of MnOy layers, as well as processes running during interaction of H_2S molecules with surface of manganese oxide. The comparative analysis was performed of sorption materials based on manganese oxide, obtained under different technological modes.

2. Experiment

Two types of sorption layers based on manganese oxide and produced by different methods are studied. In first case the sorption layer of manganese oxide was deposited from alcohol suspension of MnO_2 powder. Powder of manganese dioxide was obtained during reaction between solutions $MnSO_4$ and $KMnO_4$:

$$3MnSO_4+H_2O+2KMnO_4 \rightarrow 5MnO_2+2H_2SO_4+K_2SO_4. \tag{1}$$

The formed sediment of manganese dioxide was deposited on filter, washed with distilled water and dried at room temperature. Coating obtained by above method can be characterized as powder layer of manganese oxide.

In the second case the layer MnO_y was obtained by thermal decomposition of manganese nitrate directly on the substrate:

$$Mn(NO_3)_2 \xrightarrow{t^\circ,C} MnO_2 + 2NO_2. \tag{2}$$

The manganese oxide film is formed as follows. On the substrate layer of $Mn(NO_3)_2$ solution in ethyl alcohol with concentration 0.14 M was initially deposited, with further drying at room temperature. Then the substrates were slowly heated to temperature of 350 °C, and held at this temperature for 5 min. At that on the substrate the island structure of crystallites of manganese oxide was formed. The procedure was repeated until solid layer of MnO_y is obtained in form of thin film.

Studies of the morphology and element composition of layers MnO_y were performed by method of scanning-electron microscopy (SEM) and energy-dispersive analysis (EDA) in scanning-electron microscope Jeol JSM-6610-LV with energy-dispersive analyzer Inca-XAct.

Chemical state of manganese oxide layers before and after H_2S sorption was studied using methods of X-ray photoelectron spectroscopy (XPS) in unit Surface Science

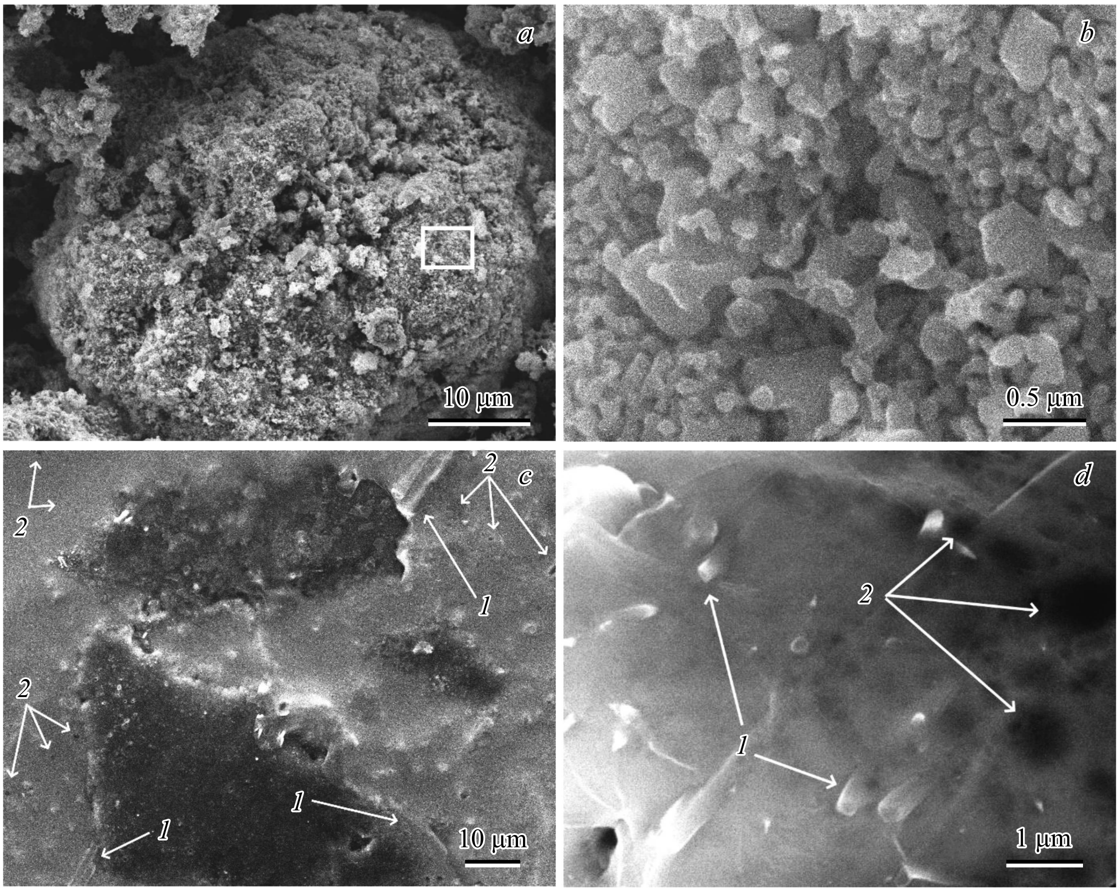

Figure 1. SEM-image of MnOy layers at different zoom: *a* and *b* — powder layer; *c* and *d* — film layer. Digits mark: *1* — tubular structures on layer surface; *2* — pores in manganese oxide layer.

Center (Riber). For X-ray radiation excitation the non-monochromatic source with Al-anode with photon energy 1486.7 eV was used. XPS spectra were measured under conditions of ultrahigh vacuum ($\sim 10^{-9}$ Torr) using analyzer MAC-2. The diameter of the X-ray beam was ~ 3 mm, the source power was 240 W. The energy resolution when registering the spectra of the core lines was ~ 0.2 eV, of panoramic spectra ~ 1.2 eV. Depth of analysis by this method was ~ 5 nm. Spectra were calibrated as per position of photoelectron line C1s (bond energy 285 ± 0.1 eV).

To study the sorption processes in the manganese oxide layers during interaction with hydrogen sulphide the samples were held in H_2S atmosphere with concentration 8000 ppm for three days. Samples after exposure were relocated directly in the loading chamber of XPS-spectrometer without long-term contact with atmosphere.

The electrophysical studies were performed using test structure containing gas-sensitive and sorption layers. As gas-sensitive element the film of nonstoichiometric tin oxide on substrate with size 10×10 mm was used. The tin oxide was obtained by method of vapor-phase deposition at thermal decomposition of tin tetrachloride:

$$SnCl_4 \cdot 5H_2O \xrightarrow{t^\circ,C} SnO_2 + 4HCl + 3H_2O. \qquad (3)$$

On surface of tin oxide film the layer of manganese oxide was deposited by the above methods. Resistance of the resistive gas-sensitive element was assessed on the basis of linear current-voltage curves (CVC) measured using the Agilent E4980A LCR meter.

To evaluate the gas-sorption characteristics of manganese oxide layers the dependence of normalized resistance of test structure (R/R_0) on time during H_2S injection into gas chamber were plotted, where R — film resistance after gas exposure, R_0 — resistance before gas exposure.

3. Results and discussion

Figure 1 presents SEM-images of layers MnO_y obtained under different modes. Samples obtained by deposition from suspension of powder MnO_y, have obvious grain structure with grain size $\sim 50-100\,\mu$m (Figure 1,*a* and *b*). At that grains have developed surface, with multiple crystallites with size 100−500 nm. At such structure the manganese oxide layer has significant area, this has positive effect on the sorption properties. Thickness of manganese oxide layer obtained by deposition from the suspension is $300-500\,\mu$m.

Manganese oxide obtained by thermal decomposition has more homogeneous structure with smeared boundaries of crystallites. This is due to that as a result of layer-by-layer deposition of manganese oxide the relief features formed at the previous stage are hidden by layer applied next. On surface the tubular structures are observed, they are formed as a result of roll-up of individual sections of layer during its formation by method of thermal decomposition. Diameter of tubular structures varies from 100 nm to 1 μm. Besides, features of the film layer of can include presence of porous structure with pore diameter of 50 nm to 1 μm.

The element chemical state of manganese oxide layers as result of hydrogen sulphide sorption was studied by XPS method. Figure 2 presents panoramic XPS-spectra of manganese oxide samples before and after exposure in vapors H_2S. spectra of initial samples (Figure 2, curves *1* and *3*) contain photoelectron lines of manganese (Mn2p, Mn3s), oxygen (O1s) and carbon (C1s) [9]. Carbon presence in sample spectra is associated with pollutants adsorption during the sample storage in air. In sample spectra after exposure in hydrogen sulphide (Figure 2, curves *2* and *4*) the photoelectron sulfur lines are observed. At that, spectrum of powder layer of manganese oxide (Figure 2, curves *2*) line S2p only (bond energy $\sim$ 165 eV) has intensity above the background level, at that in spectrum of film layer of manganese oxide the sufficiently intensive lines S2p and less intensive line S2s (bond energy $\sim$ 230 eV) present [9]. The later indicates that sorption ability of the film sample is significantly higher as compared to the powder one. Besides, in survey XPS spectrum of sample obtained by method of thermal decomposition, after exposure (Figure 2, curve *4*) the change of shape of peak Mn2p is observed indicating change in chemical state of manganese.

The results of quantitative elemental analysis of samples MnO_y, carried out on survey XPS-spectra using the elemental sensitivity coefficients are given in Table.

We see that sulfur concentration after exposure in H_2S on surface of film sample is higher by more than 4 times as compared to the powder samples. Evaluation of initial chemical state in samples as per results of quantitative analysis can indicate more oxidized state of manganese in layer of film sample. Ratio of oxygen concentration to manganese concentration for the given sample is $\sim$ 1.7, at that for powder sample $\sim$ 1.5. But presence on surface of samples of carbon pollutants slightly decrease correctness of the quantitative evaluation.

The mechanisms of interaction of hydrogen sulphide vapors with manganese oxide were determined by comparison of spectra of core levels Mn2p and S2p before and after exposure in vapors H_2S. Mn2p spectra before exposure in hydrogen sulphide vapors for both types of manganese oxide (Figure 3, curves *1* and *3*) have similar view. But spectrum of powder layer of manganese oxide (Figure 3, curve *1*) contains noticeable offset of maximum of line $Mn2p_{3/2}$ towards low bond energies, as compared to spectrum of film sample (Figure 3, curve *1*), this can indicate more oxidized state of manganese in the later case. This agrees with the results of quantitative analysis. According to literature data [9], position of maxima of line $Mn2p_{3/2}$ for the initial composites corresponds to energy range of Mn(IV) and Mn(III).

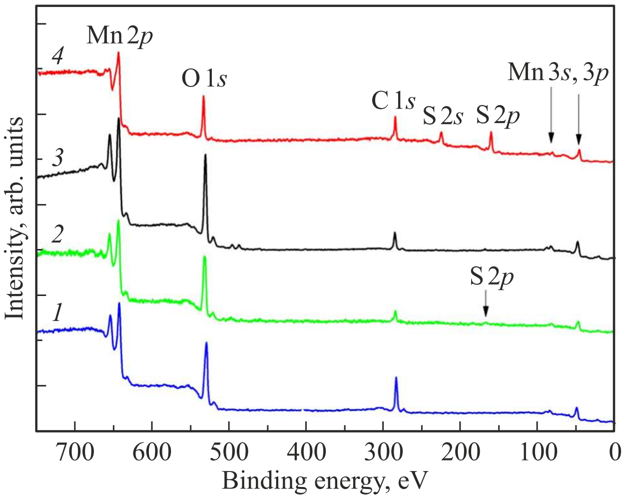

Figure 2. Survey XPS-spectra of manganese oxide samples before and after exposure in H_2S: MnO_y (powder) — curves *1* and *2* respectively; MnO_y (film) — curves *3* and *4* respectively.

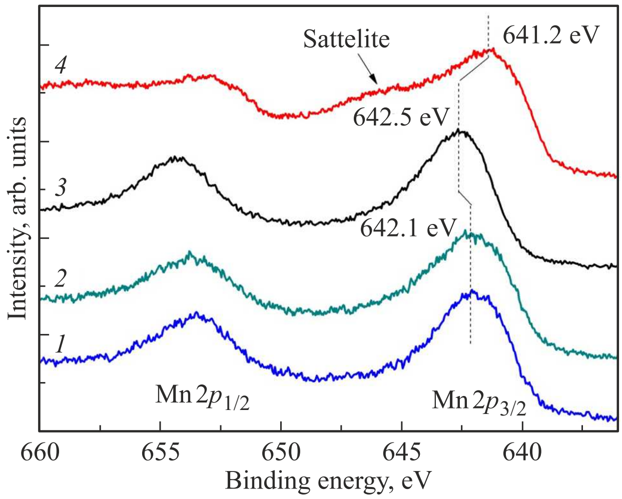

Figure 3. XPS-spectra Mn2p of manganese oxide samples before and after exposure in H_2S: layer of powder manganese oxide — curves *1* and *2* respectively; film layer of manganese oxide — curves *3* and *4* respectively.

Analysis of XPS-spectra Mn2p after holding in H_2S indicates different nature of interaction of hydrogen sulphide and manganese oxide in samples. in case of powder manganese oxide layer no significant changes in spectrum shape are observed (Figure 3, curves *1* and *2*), this can justify the physical sorption of H_2S molecules on surface of crystallites MnO_y without formation of chemical bonds with manganese. In case of manganese oxide obtained by the thermal decomposition the line offset to low bond energies

Element composition of samples before and after exposure in vapors H_2S as per XPS data

Sample	Concentration, at.%			
	[Mn]	[O]	[C]	[S]
Powder MnO_y	30.2	44.4	25.4	–
Powder MnO_y after H_2S	28.8	52.9	14.6	3.8
Film MnO_y	26.5	44.8	28.7	–
Film MnO_y after H_2S	24.5	27.7	31.8	16.0

$Mn2p_{3/2}$ from 642.5 to 641.2 eV is observed (Figure 3, curve *4*), this indicates the partial restoration of manganese. This spectrum at side of high bond energies contains intensive „arm“, which, most probably, is satellite observed in spectra of compounds of bond energy manganese [9,10]. All this indicates change in chemical state of manganese after interaction with hydrogen sulphide vapors with possible formation of manganese sulphides (MnS).

Analysis of XPS-spectra S2p (Figure 4) of samples after exposure in H_2S distinguishes two basic states of sulfur in samples under study: S^{4+} and S^{2-} [9,11]. At that in case of the powder layer of manganese oxide (Figure 4, curve *1*) in spectrum S2p state of sulfur S^{4+} prevails. This can indicate the formation of SO_2. At that, as the spectrum Mn2p analysis showed, the changes in chemical state of manganese in this sample was not observed. Hence, on surface of the powder oxide the oxidation-reduction reactions of hydrogen sulphide can run with ions of oxygen adsorbed on the surface at temperature below 100 °C in state O^{2-} [12]:

$$2H_2S(\mathrm{ads}) + 3O^{2-} \rightarrow 2H_2O + 2SO_{2(\mathrm{ads})} + 6e^-. \tag{4}$$

Low energy component of sulfur (S^{2-}) in spectrum of this sample (Figure 4, curve *1*), probably, corresponds to physically adsorbed H_2S.

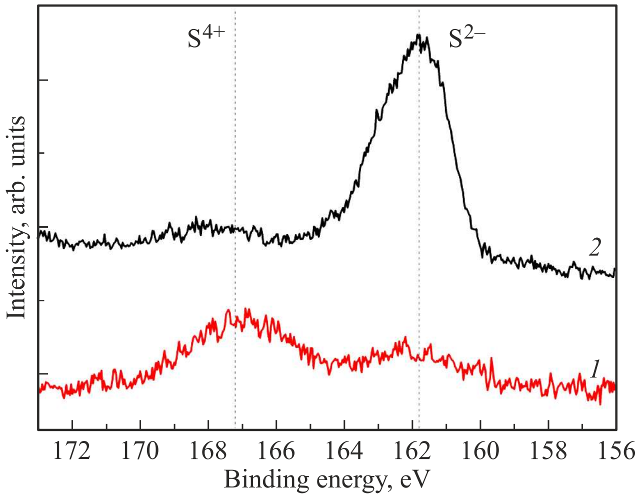

Figure 4. XPS-spectra S2p of manganese oxide samples after exposure in H_2S: curve *1* — powder layer, *2* — film layer.

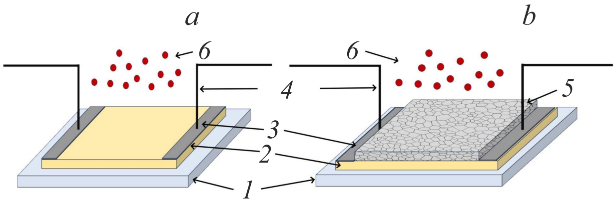

Figure 5. Diagram of experiment on evaluation of response of test structure of resistive gas sensors: *a*) without adsorbing layer; *b*) with layer MnO_y. *1* — polycrystalline glass substrate; *2* — layer of nonstoichiometric tin oxide; *3* — metal contacts; *4* — probes of metering unit; *5* — sorption layer MnO_y; *6* — molecules of gas-analyte (H_2S).

The spectrum S2p of sample obtained by thermal decomposition contains sulfur atoms predominantly in state S^{2-} (Figure 4, curve *2*). Such state of sulfur corresponds to compounds H_2S or MnS. XPS data comparison can suppose that in this case during interaction of hydrogen sulphide with surface of manganese oxide layer the chemical reaction runs, as a result of which manganese oxide is restored to sulphide (II). Therefore, the hydrogen sulphide sorption has chemical nature, and in surface the following reactions [13] can run:

$$2MnO_2 + 2H_2S_{(\mathrm{ads})} \rightarrow 2MnS + 2H_2O + O^{2-}, \tag{5}$$

$$Mn^{(+4)}O_2 + 2H_2S_{(\mathrm{ads})} + 2e^- \rightarrow Mn^{(+2)}S + 2H_2O + S^0. \tag{6}$$

To estimate applicability of manganese oxide layers synthesized by different methods the test structures of resistive gas sensors were prepared based on nonstoichiometric tin oxide coated with manganese oxide layer. These test structures were exposured in atmosphere saturated with hydrogen sulphide vapors with concentration 830 ppm H_2S at room temperature. The diagram of the experiment is shown in Figure 5.

The response of resistive gas-sensitive element before and after deposition of sorption layer MnO_y was compared as follows. Test structure was located into gas chamber, and series of resistance measurements of structure was performed before gas-analyte injection and during exposure in H_2S vapors. Concentration of gas-analyte in gas chamber, at time of measurements, was 830 ppm. After gas injection

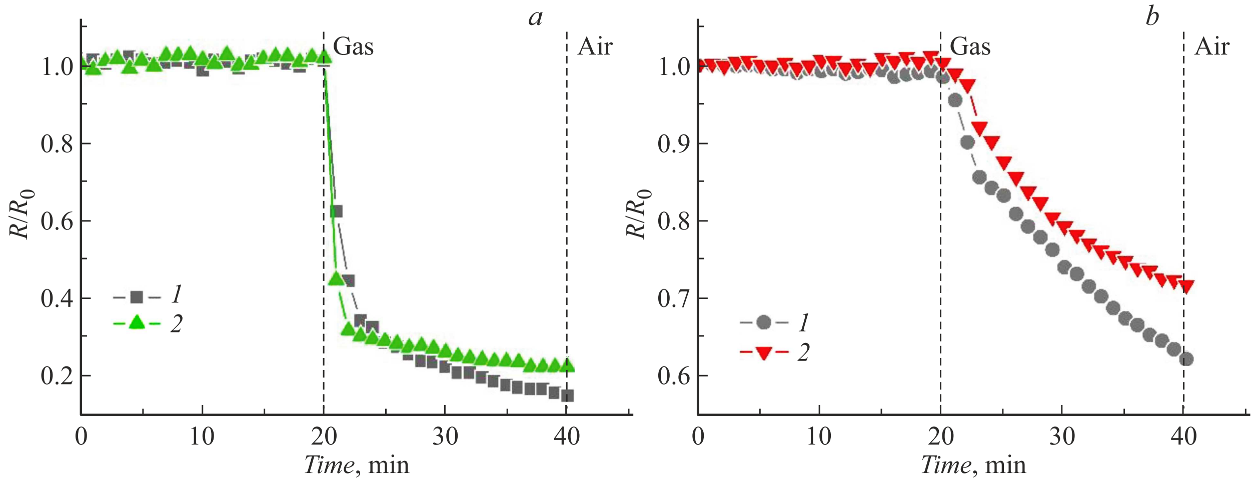

Figure 6. Change in normalized resistance (R/R_0) of test gas-sensitive element to 830 ppm H_2S with *a*) powder and *b*) film layer of manganese oxide: curve *1* — SnO_x, *2* — SnO_x/MnO_y.

into the chamber for 20 min the resistance was measured of test structures with frequency 1 measurement per minute. The measurement results are shown in graphs in Figure 6.

Different view of graphs of change of normalized resistance on time and gas injection indicate the presence in response rates and in response value for test structures. This can be associated with different structural features of film of nonstoichiometric tin oxide (oxygen concentration, heterogeneity of film thickness over surface etc.). At same time the deposition of the sorption layer does not change type of dependence of change of normalized resistance on time, this confirms absence of chemical interaction between sensitive and sorption layers. Sensor response for structure with powder layer of manganese oxide did not change as compared to initial layer of tin oxide. Considering the lateral dimensions of test structure 10 × 10 mm, we can suppose that manganese oxide layer sorbs minor concentration of hydrogen sulphide.

In case of test sensor structure with sorption layer of manganese oxide obtained the thermal decomposition, the sensor response is lower then in film of nonstoichiometric tin oxide under same conditions. Considering the geometric dimensions and features of surface relief of manganese oxide layer obtained by thermal decomposition, the results of gas sensitivity indirectly indicate more effective sorption of hydrogen sulphide molecules.

4. Conclusion

The performed studies of manganese oxide layers showed that if is obtained from solutions $MnSO_4$ and $KMnO_4$ the manganese oxide has grain structure with developed surface , and a result of interaction with vapors of hydrogen sulphide practically does not change its chemical state, at that some sulfur atoms go into state S^{4+}. Data of gas sensitive experiments do not show changes in response of test structure after deposition of powder manganese oxide layer.

The manganese oxide layer obtained by deposition from suspension catalyses the reaction of hydrogen suplhide oxidation to SO_2 via the adsorbed oxygen. At significant gas concentration all oxygen-adsorbed sites are involved in the hydrogen sulphide oxidation, and after saturation further passage and partial adsorption of H_2S occur. This is confirmed by the presence of small peak in spectrum S2p of sample of powder layer of MnO_y state S^{2-}.

In case of film sample the hydrogen sulphide is actively chemisorbed by metal atoms, as a result the film transmits the gas being studied less efficiently.

The manganese oxide layer, obtained by thermal decomposition of manganese nitrate, has less expressed relief of surface and lower layer thickness. At that during interaction with hydrogen sulphide molecules,according to XPS data the chemical interaction of MnO_y and H_2S occurs with formation of MnS. Gas sensitive measurements also show decrease in response of test structure after deposition of the manganese oxide layer.

Thus, manganese oxide layer obtained by the thermal decomposition is promising material to create gas resistive microsensors with integral layers of gas-sensitive and sorption layers.

Acknowledgments

The equipment of the Omsk Regional Center of Core Shared Research facilities of SB RAS was used in the study.

Funding

The work was performed under the state assignment of the Omsk Scientific Center of the Siberian Branch of the Russian Academy of Sciences (project registration number 121021600004-7).

Conflict of interest

The authors declare that they have no conflict of interest.

References

[1] C. Pijolat, B. Riviere, M. Kamionka, J.P. Viricelle, P. Breuil. J. Mater. Sci. **38**, *21*, 4333 (2003). https://doi.org/10.1023/A:1026387100072

[2] C. Zhang, A. Boudiba, C. Navio, M.-G. Olivier, R. Snyders, M. Debliquy. Sensors. Actuators B **161**, *1*, 914 (2012). https://doi.org/10.1016/j.snb.2011.11.062

[3] L. Bigiani, D. Zappa, C. Maccato, E. Comini, D. Barreca, A. Gasparotto. Appl. Surf. Sci. **512**, 145667 (2020). https://doi.org/10.1016/j.apsusc.2020.145667

[4] L. Bigiani, D. Zappa, Ch. Maccato, A. Gasparotto, C. Sada, E. Comini, D. Barreca. Adv. Mater. Interfaces **6**, 1901239 (2019). https://doi.org/10.1002/admi.201901239

[5] C. Zhang, J. Zheng, S. Su, Y. Jin, Z. Chen, Y. Wang, J. Xu. J. Hazard. Mater. **471**, 134402 (2024). https://doi.org/10.1016/j.jhazmat.2024.134402

[6] X. Zheng, G. Zhang, Z. Yao, Y. Zheng, L. Shen, F. Liu, Y. Cao, S. Liang, Y. Xiao, L. Jiang. J. Hazard Mater **411**, 125180 (2021). https://doi.org/10.1016/j.jhazmat.2021.125180

[7] A.A. Edathil, P. Kannan, F. Banat. Environmental Pollution **266**, *Part 3*, 115218 (2020). https://doi.org/10.1016/j.envpol.2020.115218

[8] L.-J. Wang, H.-L. Fan, J. Shangguan, E. Croiset, Z. Chen, H. Wang, J. Mi. ACS Appl. Mater. Interfaces. **6**, *23*, 21167 (2014). https://doi.org/10.1021/am506077j

[9] Table of elements. Manganese. Manganese X-ray photoelectron spectra, manganese electron configuration, and other elemental information. Internet database. Thermo Fisher Scientific. https://www.thermofisher.com/ru/ru/home/materials-science/learning-center/periodic-table/transition-metal/manganese.html

[10] M.C. Biesinger, B.P. Payne, A.P. Grosvenor, L.W.M. Lau, A.R. Gerson, R.St.-C. Smart. Appl. Surf. Sci. **257**, *7*, 2717 (2011)

[11] Y.-C. Lin, Y.-Y. Chen, B.-Y. Yu, W.-C. Lin, C.-H. Kuo, J.-J. Shyue. Analyst **134**, *5*, 945 (2009). https://doi.org/10.1039/b814729a

[12] P.S. Kolhe, S.G. Kulkarni, N. Maiti, K.M. Sonawane. Appl. Phys. A **125**, *5*, 372 (2019). https://doi.org/10.1007/s00339-019-2663-0

[13] A. Ahmed, S. Elkatatny, S.A. Onaizi. ACS Omega **8**, *49*, 46738 (2023). https://doi.org/10.1021/acsomega.3c05740

Translated by I.Mazurov